Breathing mechanism of a cracked rotor subject to non-trivial mass unbalance

Joseph Patrick SPAGNOL[1]; Helen WU[2]

[1, 2] University of Western Sydney, Australia

ABSTRACT

The effects of dynamic loading on crack breathing mechanisms are not yet thoroughly examined in literature. This paper introduces a parameter relating crack direction to bending load direction in order to model breathing behaviour of fatigue cracks subject to mass unbalance. Crack states (open, partial and closed) for shafts subject to weight-to-unbalance force ratios of 0.5, 1 and 2 and unbalance orientation angles of 0°, 45°, 90°, 135° and 180° were sometimes seen to be non-sequential or unchanging at particular crack depths. Additionally, the effects of varying unbalance angles and crack depth ratios on breathing mechanisms were also examined. An area moment of inertia method was used to develop a time-varying global stiffness matrix for each case and the results were found to be highly agreeable with the crack breathing behaviour in each case.

Keywords: Crack breathing, Unbalance, Cracked shaft, Fatigue crack, Finite Element Method

1. INTRODUCTION

Fatigue cracks and mass unbalance are amongst the primary causes of abnormal vibration patterns in rotating machinery. Crack development in rotors subject to cyclic loading is an inevitable phenomenon that is caused by high stress concentrations in areas of sharp geometry changes and regions of material defects. Due to the rapid yet subtle nature of shaft cracks, monitoring and early diagnosis play a pivotal role in preventing fractures and in ultimately avoiding catastrophic failure of machinery. This complication is further exacerbated by the difficulty to inspect shafts whilst in operation. As such, recent research trends have focused on the speed, location and depth of cracks in the interest of predictive modelling (1).

Cracked shafts subjected to alternating stresses elucidate a complex, non-linear behaviour known as crack breathing. This breathing mechanism is a result of stress and strain distribution in the region of the crack where, typically, compressive stresses correspond to the closing of a crack and tensile stresses to an opening of the crack.

Breathing functions that accurately characterise breathing behaviour can be developed using a number of models. The switching crack model as seen in (2-5) is a simplified crack breathing model that assumes breathing behaviour to be binary (open or closed). It is suggested in (6) that switching crack models are associated with quasi-periodic vibrations that are not seen in experimental testing. A more accurate method commonly seen in literature is one that utilises strain energy release rate (SERR) theory (7-9). SERR relates changes in the stress intensity factor at the crack tip to the change in overall shaft stiffness. Another technique used in literature exploits the change in area moment of inertia of the cracked shaft to develop time varying stiffness matrix equations. Such a method is seen in (1, 10-16) and further developed in (15). The authors of (17) implement the area moment of inertia models in (14-16) to perform a parametric stability analysis on cracked Jeffcott rotor using Floquet theory.

Many papers relating to the crack breathing mechanism of shafts opt to not consider mass unbalance but have provided a number of techniques to study the breathing mechanism. Amongst these papers (10-12, 18, 19) it is typically assumed that the static bending of the shaft dominates the dynamic

[1] 17203669@student.uws.edu.au

[2] helen.wu@uws.edu.au

loading of the shaft. This assumption is valid for large rotor systems with negligible mass unbalance, but for vertical rotors or lightweight horizontal rotors this assumption reduces the precision of theoretical models.

A notable source that examines crack breathing and unbalance is seen in (20). The assumption of weight dominance is removed in order to analyse the effects of unbalance orientation angle β on the dynamic response of a cracked rotor. Determination of stability, critical speed and peak response of the rotor are also examined. The authors, however, do not provide deep insight into crack state variations based on other unbalance parameters.

Diagnosis and modeling of cracked rotors with mass unbalance using modal expansion and a reduced basis dynamic expansion (RBDE) method is seen in (21). Depictions of the crack breathing mechanisms were absent from the study. Finite element procedures used in (22) shed light upon the effects of crack orientation and crack shape on the crack breathing mechanism.

2. METHODOLOGY

2.1 Crack Breathing Model

A geometry approach for calculating the effectual loading angle was developed for this paper and is seen in Figure 1. The bending force direction δ and magnitude *R* is determined as the vector sum angle of the static weight force F_g and the unbalance force F_{me} which rotates at a fixed angle β relative to the crack direction. The crack direction angle Ωt is considered to be zero when it is parallel to the negative Y-axis.

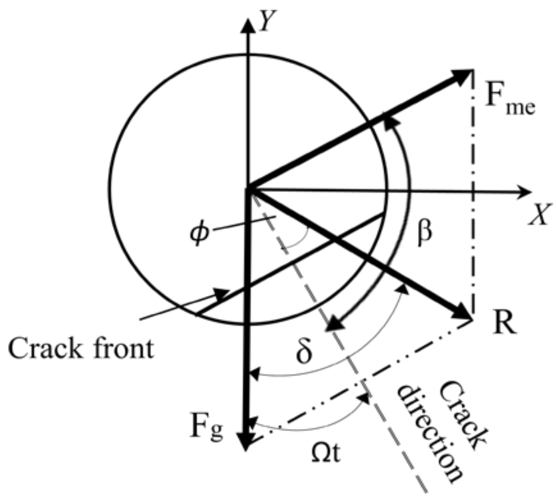

Figure 1 – Cross sectional diagram of a cracked element

The effectual loading angle ϕ is then calculated by

$$\emptyset = \Omega t - \tan^{-1}\left[\frac{\sin(\Omega t + \beta)}{\cos(\Omega t + \beta) + \eta}\right] \quad (1)$$

where ϕ is defined as the angle difference between the crack direction angle and the resultant force angle, and η is the ratio between the weight force and mass unbalance force.

Crack breathing functions were then adopted from (15) to determine the state of the crack i.e. fully open, partial or fully closed by replacing Ωt with ϕ in each equation. For the region $\theta_1 < \phi < 2\pi - \theta_1$ the crack is fully open. Similarly, the region $\theta_2 < \phi < 2\pi - \theta_2$ describes the shaft rotation angles for when the crack is completely closed. When the effectual loading angle is outside of these regions the crack is considered to be partially open/closed.

Figure 2 shows the relationship between the effectual loading angle and the shaft rotation angle for a non-dimensional crack depth of 0.4. When the shaft rotates between 339.4° and 63.7° from its original position the crack is completely open, similarly when the shaft is between 119.5° and 193.3° the crack is fully closed. Outside of these regions the crack is partially open and partially closed. This breathing behaviour is more clearly depicted in the accompanying pie chart. Discontinuity exists at Ωt = 30° due to the crack direction angle transitioning from following to leading the bending direction.

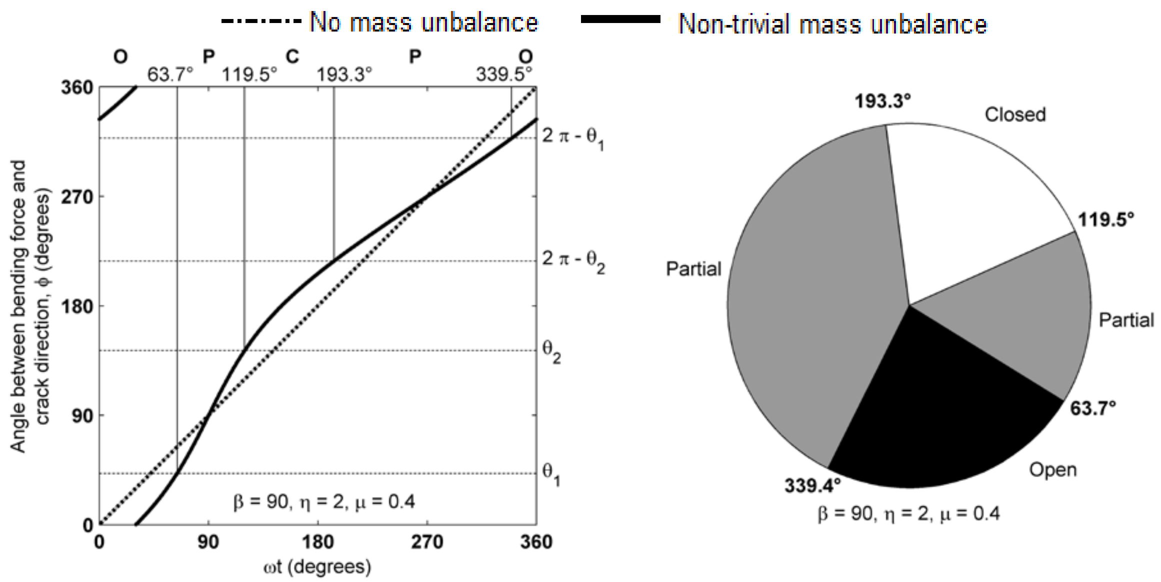

Figure 2 – Effectual loading angle versus shaft rotation for $\beta = 90^{\circ}$, $\eta = 2$ and $\mu = 0.4$

Regardless of crack depth, cases with no mass unbalance such as the one seen in Figure 3 will present a breathing behaviour that could be described as being symmetrical and sequential. For the purpose of this paper sequential crack breathing behaviour refers to the orderly transition of a fatigue crack from open to partial, partial to closed, closed to partial and finally partial to open states in one period of the shaft rotation. Whilst the particular case in Figure 2 is sequential, it is however not symmetrical due to the relationship between the effectual loading angle and the shaft rotation being non-linear. As a result, the case seen in Figure 2 has a reduced angle range for the first partial state as compared to the no unbalance case, with a range of 55.8° and 100.8°, respectively. Moreover, the second partial state occurs over a much wider angle range of 146.6° as compared to the 100.8° for the zero mass unbalance case. The closed and open angle ranges of the aforementioned cases are similar, but it should noted that this is coincidental and not indicative of open and closed angle ranges for other mass unbalance cases.

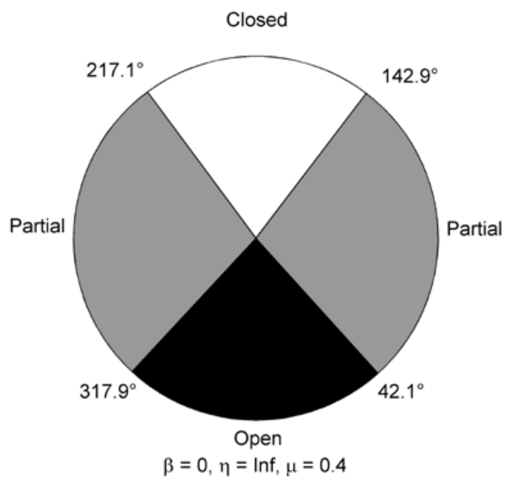

Figure 3 – Crack breathing behaviour of a shaft with no mass unbalance

Two interesting instances of dynamic loading on crack breathing are seen in Figure 4 and Figure 5. These particular cases amongst many more challenge the paradigm seen in literature for crack breathing behaviour. Both cases are seen to be non-sequential and non-linear; even more so the case seen in Figure 4 does not transition out of the closed state. It is possible for the crack to remain fully closed throughout the entire shaft rotation if the effectual loading angle ϕ remains within the region $\theta_2 < \phi < 2\pi - \theta_2$. Such a case could render crack detection through area moment of inertia changes as being virtually impossible.

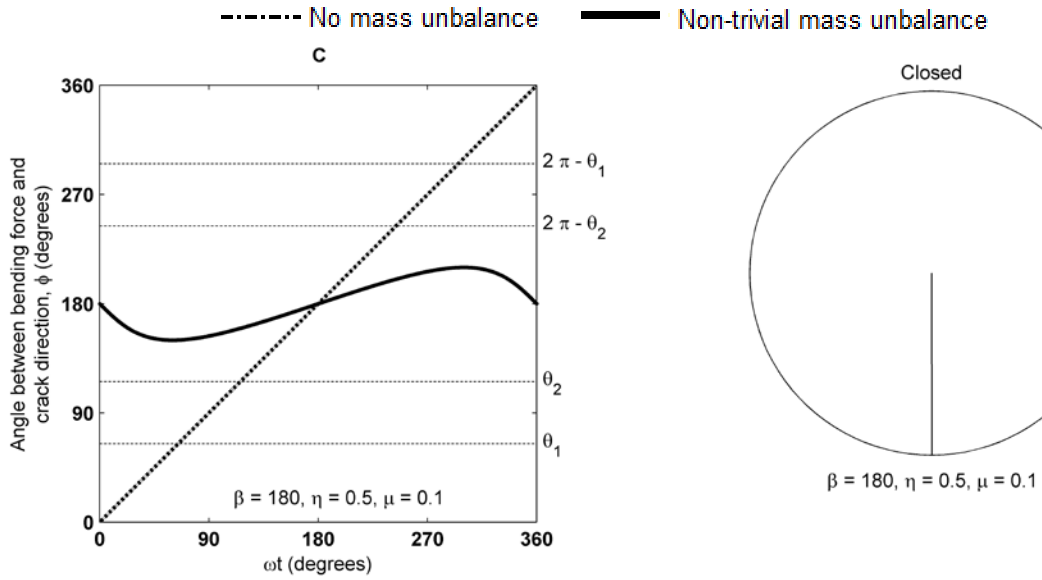

Figure 4 – Effectual loading angle versus shaft rotation for β = 180, η = 0.5 and μ = 0.1

The case seen in Figure 5 demonstrates a quintessential example of non-sequential crack breathing behaviour. At Ωt = 0 the crack is in a partially open/closed state up to 39.6° where it is completely open until 90.4°. Instead of transitioning into another partial state the crack closes for a small range of angles before entering a partial state once again.

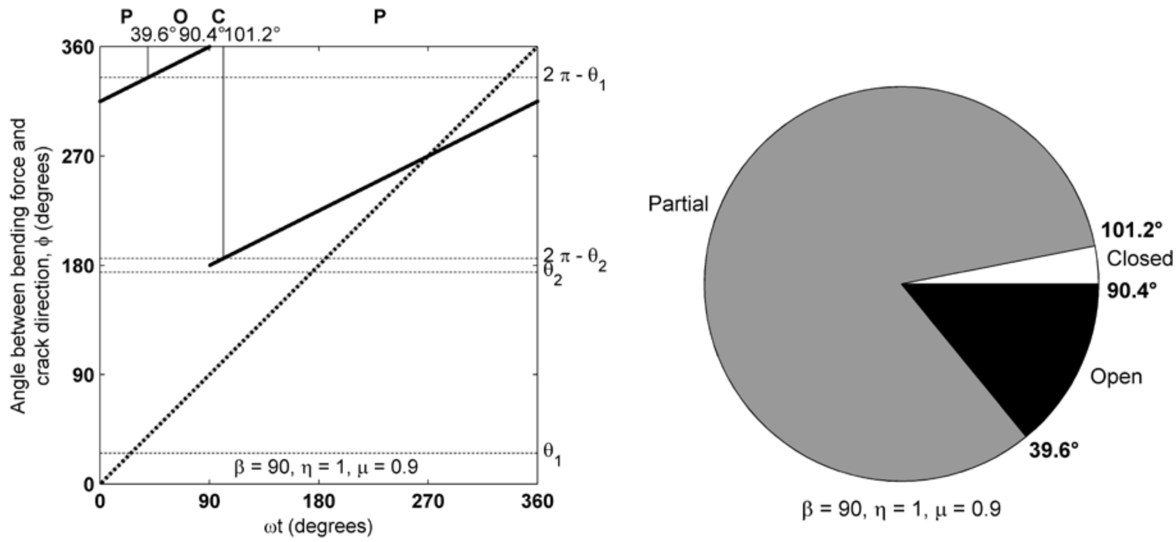

Figure 5 – Effectual loading angle versus shaft rotation for β = 90, η = 1 and μ = 0.9

It is highly evident that the crack breathing behaviour of a shaft subject to non-trivial unbalance may greatly differ from cases with no mass unbalance. Consequently, the new crack breathing models must be employed to accurately depict the true vibration behaviour and to ultimately solve the equations of motion for the rotor system. It should also be mentioned that the crack breathing behaviour for combinations of β = 0°, 45°, 90°, 135° and 180° and η = 0.5, 1 and 2 at different crack depths were also studied but will not be discussed.

2.2 Area Moment of Inertia

Before information can be obtained about the vibration of the rotor system the stiffness matrix associated with the breathing fatigue crack must be determined. As cracks transition between open and closed states the overall stiffness of the shaft changes accordingly where a fully open crack corresponds to minimum shaft stiffness and a fully closed crack corresponds to maximum shaft stiffness. The severity of stiffness changes due to cracking can be accurately reflected by the change in area moment of inertia of the non-cracked element. As such, the local time-varying stiffness matrix was determined using the approximate area moment of inertia calculations developed in (15). Replacing the shaft rotation angle by the effectual load angle was necessary to include the effects of rotational unbalance.

Figure 6 shows a strong correlation between approximate area moment of inertia and the breathing mechanism seen in Figure 2. When the crack is in a fully closed state the area of the non-cracked element is equal to the cross-sectional area of the whole shaft i.e. at a maximum value from 119.5° to 193.3°. Similarly, the area moment of inertia is lowest when the crack is fully open (339.4° to 63.7°).

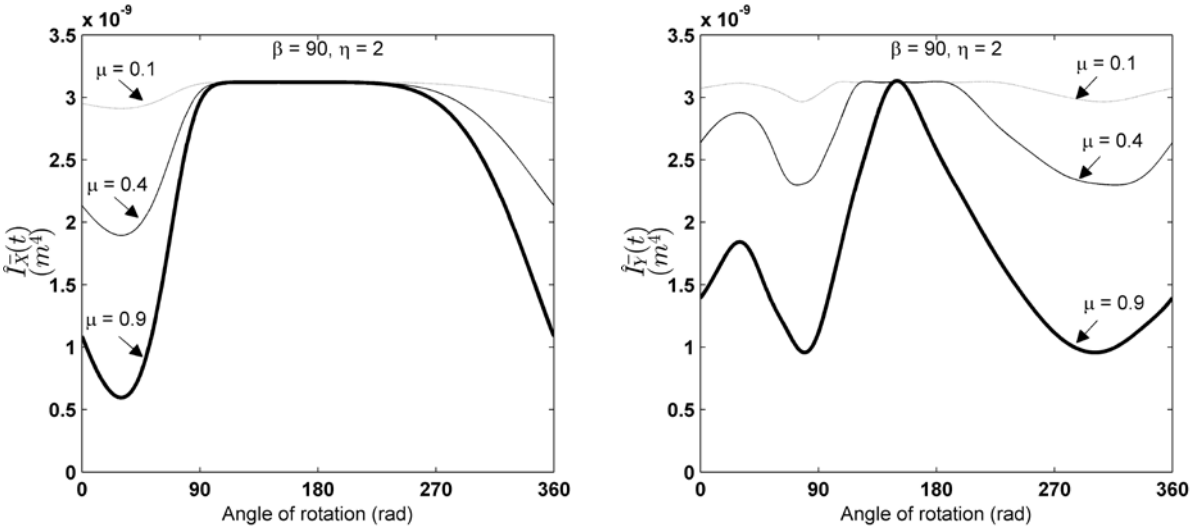

Figure 6 – Approximate change in area moment of inertia of the cracked element for β = 90, η = 2 (left) about X-axis, (right) Y-axis

The local stiffness matrix of the cracked element is given by

$$
\mathrm{k_{ce}} = \frac{\mathrm{E}}{\mathrm{l}^3}\begin{bmatrix}
12\hat{I}_{\bar{X}} & 0 & 0 & 6l\hat{I}_{\bar{X}} & -12l\hat{I}_{\bar{X}} & 0 & 0 & 6l\hat{I}_{\bar{X}} \\
0 & 12\hat{I}_{\bar{Y}} & -6\hat{I}_{\bar{Y}} & 0 & 0 & -12\hat{I}_{\bar{Y}} & -6l\hat{I}_{\bar{Y}} & 0 \\
0 & -6l\hat{I}_{\bar{Y}} & 4l^2\hat{I}_{\bar{Y}} & 0 & 0 & 6l\hat{I}_{\bar{Y}} & 2\mathrm{l}^2\hat{I}_{\bar{Y}} & 0 \\
6l\hat{I}_{\bar{X}} & 0 & 0 & 4l^2\hat{I}_{\bar{X}} & -6l\hat{I}_{\bar{X}} & 0 & 0 & 2l^2\hat{I}_{\bar{X}} \\
-12l\hat{I}_{\bar{X}} & 0 & 0 & -6l\hat{I}_{\bar{X}} & 12\hat{I}_{\bar{X}} & 0 & 0 & -6l\hat{I}_{\bar{X}} \\
0 & -12\hat{I}_{\bar{Y}} & 6l\hat{I}_{\bar{Y}} & 0 & 0 & 12\hat{I}_{\bar{Y}} & 6l\hat{I}_{\bar{Y}} & 0 \\
0 & -6l\hat{I}_{\bar{Y}} & 2l^2\hat{I}_{\bar{Y}} & 0 & 0 & 6l\hat{I}_{\bar{Y}} & 4\mathrm{l}^2\hat{I}_{\bar{Y}} & 0 \\
6l\hat{I}_{\bar{X}} & 0 & 0 & 2l^2\hat{I}_{\bar{X}} & -6l\hat{I}_{\bar{X}} & 0 & 0 & 4l^2\hat{I}_{\bar{X}}
\end{bmatrix} \tag{2}
$$

where l is the length of the finite element containing the crack, $\hat{I}_{\bar{X}}$ and $\hat{I}_{\bar{Y}}$ are the approximate moment of inertias about the fixed X-axis and fixed Y-axis, respectively.

2.3 Finite Element Model

A finite element (FE) approach is utilised to determine the time varying global stiffness matrix of the cracked disk-shaft system. The rotor was discretised into N = 18 elements, where the shaft was grounded at nodes 1 and 19 by symmetric stiffness and damping coefficient bearings. Additionally, the unbalanced disk was mounted at node 10 and the crack was located in the 10^{th} element. MATLAB was used to successfully assemble the global stiffness, damping and mass matrices.

The FE model can be written as a non-homogenous second-order differential equation with viscous damping

$$
\mathbf{M}\ddot{q} + \mathbf{G}\dot{q} + \mathbf{K}q = F_1\cos(\Omega t) + F_2\sin(\Omega t) + F_g \tag{3}
$$

where **M, G** and **K** are the 4(N+1) × 4(N+1) global mass, gyroscopic/damping and cracked stiffness matrices, respectively. q is the 4(N+1) rotor displacement vector, $F_1\cos(\Omega t) + F_2\sin(\Omega t)$ is the sum of unbalance forces, where the magnitude of F_1 and F_2 is equal to $me\omega^2$. F_g is the weight force of the shaft and disk.

3. SUMMARY AND FUTURE WORK

The effect of various rotor mass unbalance magnitudes and orientations on the crack breathing mechanism of shafts with non-dimensional crack depths of 0.1, 0.4 and 0.9 were examined. Crack behavior was seen to be non-symmetrical, non-sequential or unchanging in most cases. Area moment of inertia models of the cracked rotor were used to determine the time-varying stiffness matrix for the entire disk-shaft system.

A portion of future research efforts will be dedicated in using the developed FE model to determine the orbital and frequency response for each mass unbalance case. Such results will be compared to the orbital and frequency response of a cracked shaft with negligible mass unbalance. Additionally, the mode shapes and deflection of the shaft will be modelled and all of the results will be validated through simulatory and experimental means. The newly developed methods will be used in the analysis of real machines to detect fatigue cracks, in particular the depth and location of the crack along the rotor.

REFERENCES

1. Bachschmid N, Pennacchi P, Tanzi E. Cracked Rotors: A Survey on Static and Dynamic Behaviour Including Modelling and Diagnosis: Springer Berlin Heidelberg; 2010.
2. Shravankumar C, Tiwari R. Identification of stiffness and periodic excitation forces of a transverse switching crack in a Laval rotor. Fatigue & Fracture of Engineering Materials & Structures. 2013;36(3):254-69.
3. AL-Shudeifat MA, Butcher EA. On the dynamics of a beam with switching crack and damaged boundaries. Journal of Vibration and Control. 2013;19(1):30-46.
4. Gasch R. Dynamic behaviour of the Laval rotor with a transverse crack. Mechanical Systems and Signal Processing. 2008;22(4):790-804.
5. Pu YP, Chen J, Zou J, Zhong P. QUASI-PERIODIC VIBRATION OF CRACKED ROTOR ON FLEXIBLE BEARINGS. Journal of Sound and Vibration. 2002;251(5):875-90.
6. Patel TH, Darpe AK. Influence of crack breathing model on nonlinear dynamics of a cracked rotor. Journal of Sound and Vibration. 2008;311(3–5):953-72.
7. Darpe AK, Gupta K, Chawla A. Transient response and breathing behaviour of a cracked Jeffcott rotor. Journal of Sound and Vibration. 2004;272(1–2):207-43.
8. Jun OS, Eun HJ, Earmme YY, Lee CW. Modelling and vibration analysis of a simple rotor with a breathing crack. Journal of Sound and Vibration. 1992;155(2):273-90.
9. Rubio L, Fernández-Sáez J. A new efficient procedure to solve the nonlinear dynamics of a cracked rotor. Nonlinear Dyn. 2012;70(3):1731-45.
10. Bachschmid N, Pennacchi P, Tanzi E. Some remarks on breathing mechanism, on non-linear effects and on slant and helicoidal cracks. Mechanical Systems and Signal Processing. 2008;22(4):879-904.
11. Sinou J-J, Lees AW. A non-linear study of a cracked rotor. European Journal of Mechanics - A/Solids. 2007;26(1):152-70.
12. Sinou J-J. Effects of a crack on the stability of a non-linear rotor system. International Journal of Non-Linear Mechanics. 2007;42(7):959-72.
13. Sinou JJ, Lees AW. The influence of cracks in rotating shafts. Journal of Sound and Vibration. 2005;285(4–5):1015-37.
14. Al-Shudeifat MA. On the finite element modeling of the asymmetric cracked rotor. Journal of Sound and Vibration. 2013;332(11):2795-807.
15. Al-Shudeifat MA, Butcher EA. New breathing functions for the transverse breathing crack of the cracked rotor system: Approach for critical and subcritical harmonic analysis. Journal of Sound and Vibration. 2011;330(3):526-44.
16. Al-Shudeifat MA, Butcher EA, Stern CR. General harmonic balance solution of a cracked rotor-bearing-disk system for harmonic and sub-harmonic analysis: Analytical and experimental approach. International Journal of Engineering Science. 2010;48(10):921-35.
17. Guo C, Al-Shudeifat MA, Yan J, Bergman LA, McFarland DM, Butcher EA. Stability analysis for transverse breathing cracks in rotor systems. European Journal of Mechanics - A/Solids. 2013;42(0):27-34.
18. Yan G, De Stefano A, Matta E, Feng R. A novel approach to detecting breathing-fatigue cracks based on

dynamic characteristics. Journal of Sound and Vibration. 2013;332(2):407-22.
19. Darpe AK. A novel way to detect transverse surface crack in a rotating shaft. Journal of Sound and Vibration. 2007;305(1–2):151-71.
20. Cheng L, Li N, Chen X-F, He Z-J. The influence of crack breathing and imbalance orientation angle on the characteristics of the critical speed of a cracked rotor. Journal of Sound and Vibration. 2011;330(9):2031-48.
21. Sekhar A. Identification of Unbalance and Crack Acting Simultaneously in a Rotor System: Modal Expansion versus Reduced Basis Dynamic Expansion. Journal of Vibration and Control. 2005;11(9):1125-45.
22. Georgantzinos SK, Anifantis NK. An insight into the breathing mechanism of a crack in a rotating shaft. Journal of Sound and Vibration. 2008;318(1–2):279-95.